CORE
Metadata, citation and similar papers at core.ac.uk
Provided by Missouri University of Science and Technology (Missouri S&T): Scholars' Mine

Missouri University of Science and Technology
Scholars' Mine

Materials Science and Engineering Faculty Research & Creative Works

Materials Science and Engineering

01 Nov 2000

High Strain Rate Superplasticity in Microcrystalline and Nanocrystalline Materials

S. X. McFadden

A. V. Sergueeva

Rajiv S. Mishra
Missouri University of Science and Technology

A. K. Mukherjee

Follow this and additional works at: https://scholarsmine.mst.edu/matsci_eng_facwork

 Part of the Materials Science and Engineering Commons

Recommended Citation

S. X. McFadden et al., "High Strain Rate Superplasticity in Microcrystalline and Nanocrystalline Materials," *Materials Science & Technology*, Maney Publishing, Nov 2000.

This Article - Journal is brought to you for free and open access by Scholars' Mine. It has been accepted for inclusion in Materials Science and Engineering Faculty Research & Creative Works by an authorized administrator of Scholars' Mine. This work is protected by U. S. Copyright Law. Unauthorized use including reproduction for redistribution requires the permission of the copyright holder. For more information, please contact scholarsmine@mst.edu.

High strain rate superplasticity in microcrystalline and nanocrystalline materials

S. X. McFadden, A. V. Sergueeva, R. S. Mishra, and A. K. Mukherjee

Superplasticity has evolved to become a significant industrial forming process. The phenomenon of superplasticity is explored at high strain rates where it is economically more attractive. True tensile superplasticity has been demonstrated in nanocrystalline materials. The difference in the details of superplasticity between the nanocrystalline and microcrystalline state is emphasised. **MST/4785**

The authors are in the Department of Chemical Engineering and Material Science, University of California, Davis, CA 95616, USA. *Contribution to the 'Structure of materials' section of Materials Congress 2000 organised by IoM at Cirencester on 12–14 April 2000.*
© *2000 IoM Communications Ltd.*

Published by Maney Publishing (c) IOM Communications Ltd

High strain rate superplasticity in microcrystalline matrix

During the early years of development of this field the grain sizes used to be ~ 15 μm and the optimum strain rate used to be $\sim 10^{-4}$ s^{-1} (especially for Al alloys). With development of processing methods to produce ultrafine grain size materials, it has been possible to increase the optimum forming rates to approximately $10^{-1}-10^{-2}$ s^{-1}. In this range, high strain rate superplasticity (HSRS) has been explored extensively in recent years.

The general features of HSRS are as follows:

(i) the parametric dependencies tend to be influenced by the reinforcement size and grain size
(ii) the optimum superplastic temperature changes with the matrix material
(iii) the optimum superplastic conditions can be significantly altered by prior thermomechanical processing.[1]

The natural question that arises is whether the rate controlling mechanism is the same for HSRS in all materials. The present study shows that the size of second phase particles influences the parametric dependencies, particularly the high activation energy for HSRS for large reinforcing particle sizes. The results are explained on the basis of a change in the rate controlling mechanism with particle size.

The present analysis is based on the existence of a threshold stress for HSRS in dispersion strengthened materials. The variation of the activation energy (calculated after taking into account the presence of a temperature dependent threshold stress) with particle size is plotted in Fig. 1 for a number of mechanically alloyed Al matrix composites. The important observation that is apparent from Fig. 1 is the change in activation energy for alloys with bigger particle sizes. It is, therefore, appropriate to examine the role of particle size on the accommodation process during superplasticity.

Figure 2*a* shows the classic concept of slip accommodation during grain boundary sliding. This has been shown to be applicable for a number of materials,[3] however for materials with second phase particles the process is altered as shown in Fig. 2*b*. The particles at grain boundaries (e.g. particle marked P_{gb} in Fig. 2*b*) impede the grain boundary sliding and lead to stress concentration. This stress concentration must be lowered for continuous sliding to take place and to avoid cavity nucleation. The stress relaxation can occur by diffusional flow of atoms around the particles as depicted in Fig. 2*b*. If the rate of diffusional relaxation is fast enough to remove the stress buildup, then the overall grain boundary sliding would not be influenced parametrically. The rate of such diffusional relaxation of stress concentration has been calculated by Koeller and Raj[4] and by Mori *et al.*[2] In addition, Koeller and Raj[4] have pointed out that the increase in stress at the particle matrix interface above a critical strain rate may result in decohesion at the interface leading to formation of voids, and a consequent loss of ductility. The critical strain rate for cavity nucleation is given by

$$\dot{\varepsilon}_c \geqslant C\,\frac{(1-\nu)[1-2\nu+(2/\nu)]}{(5/6-\nu)^2}\left(\frac{G\Omega}{kT}\right)\left(\frac{V_f\delta D_g}{d_p^3}\right) \qquad (1)$$

where $\dot{\varepsilon}_c$ is the critical strain rate, ν is the Poisson's ratio, G is the shear modulus, Ω is the atomic volume, k is a constant, T is the absolute temperature, V_f is the volume fraction of particles, d_p is the particle diameter, and δ is the grain boundary width.[3] The numerical constant C has the value of 118 in the work of Koeller and Raj.[3] Subsequently, Mori *et al.*[4] found that a more rigorous analysis results in a lower value for the constant C equal to 9. This equation is derived on the basis of interfacial diffusional relaxation.

The applicability of diffusional relaxation on the onset of HSRS is evaluated in alloy MA6000 (an ultrafine oxide dispersion strengthened Ni based alloy). Taking values of

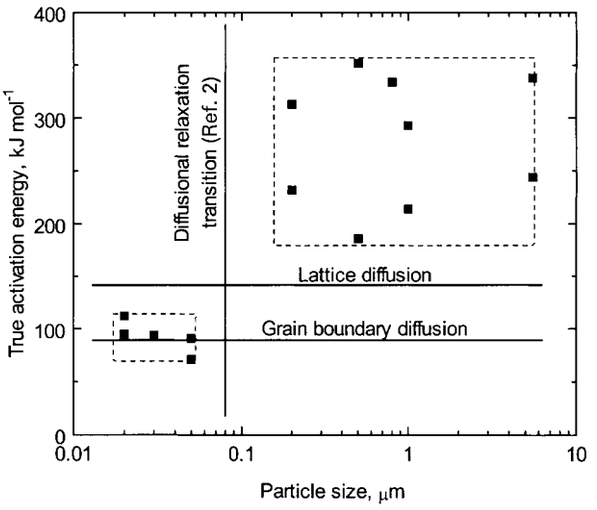

1 Variation of true activation energy with particle size for mechanically alloyed Al alloys and Al matrix composites: note that change can be predicted by diffusional relaxation models

 ISSN 0267–0836

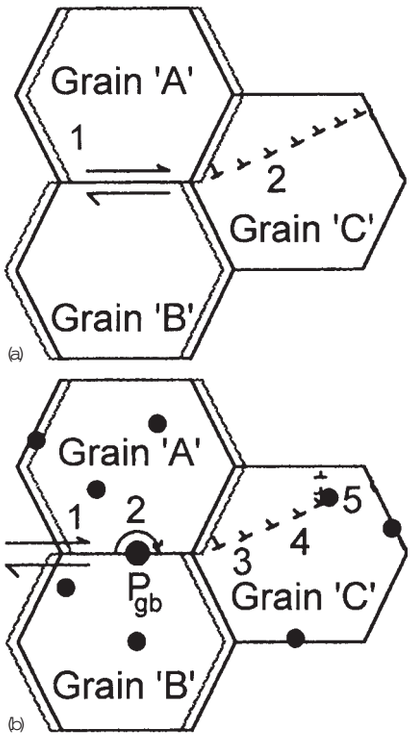

a typical micrograin superplasticity in single phase material or when all phases are deformable; 1: grain boundary sliding; 2: dislocation accommodation; *b* modification of grain boundary sliding and dislocation movement during slip accommodation due to presence of second phase particles; 1: grain boundary sliding; 2: diffusional accommodation at particle; 3: dislocation accommodation; 4: dislocation glide; 5: dislocation climb over particle

2 Effect of second phase particles on slip accommodation during grain boundary sliding

$v=0{\cdot}33$, $V_f=0{\cdot}025$, $d_p=10$ nm, D_v, G, and Ω from Frost and Ashby,[5] $\dot{\varepsilon}_c=0{\cdot}3\ s^{-1}$, and the constant $C=9$ (according to Mori *et al.*[4]), the critical temperature at which the diffusional relaxation rate is fast enough to relax the stress buildup comes out to be $\sim$1150 K. The prediction of equation (1) is compared with the data of Singer and Gessinger[6] for alloy MA6000 in Fig. 3. It can be noted that the increase in observed ductility agrees well with the prediction of the diffusional relaxation model. Another way to verify the applicability of this concept is to calculate the

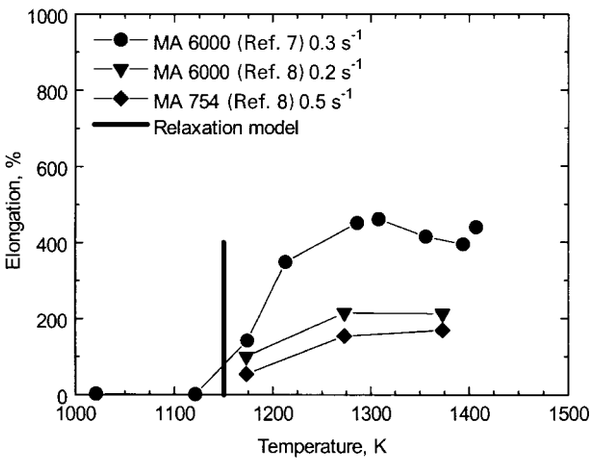

3 Onset of high strain rate superplasticity in mechanically alloyed Ni based alloys as function of temperature

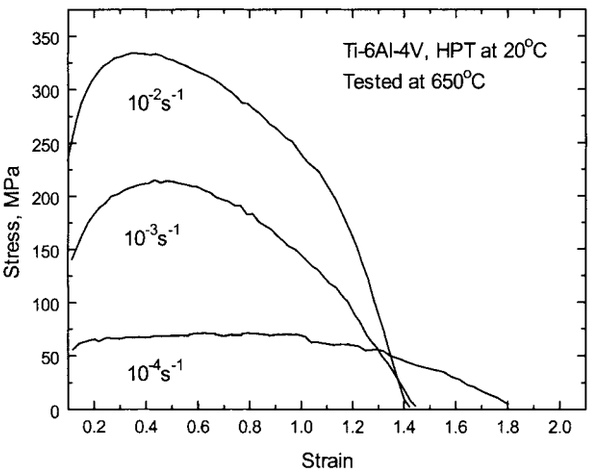

4 Typical stress–strain curves for Ti–6Al–4V processed by high pressure torsion straining (HPTS)

critical particle size for a given temperature and strain rate below which diffusional relaxation will be adequate. The result of such a calculation for Al alloys is incorporated in Fig. 1 (at 773 K, $V_f=0{\cdot}1$, and $\dot{\varepsilon}_c=100\ s^{-1}$, *see* Ref. 9). The critical particle size comes out to be 0·08 μm, using the constant $C=9$ from Mori *et al.*[2] in equation (1). The change in activation energy agrees with the critical particle size for relaxation by grain boundary diffusion, according to this equation.

In the case of metal matrix composites, the microstructure is quite different. This situation has been treated in detail by Mukherjee *et al.*[1] and will not be treated any further in the present study. However, the analysis in Ref. 1 does explain the experimentally observed activation energy that is often much higher than that for volume diffusion of the matrix.

High strain rate superplasticity in submicrocrystalline matrix

Experiments on superplastic materials have demonstrated that a reduction in grain size has the potential of both decreasing the temperature and increasing the strain rate associated with optimum superplastic flow.[10–14] High strain rate superplasticity has been evaluated by the present authors in a Ti–6Al–4V alloy processed by high pressure torsion (HPT) straining at different temperatures. This severe plastic deformation (SPD) method allows the production of specimens with no residual porosity and with grain sizes of 100 nm or less.[15]

The analysis of HPT Ti–6Al–4V alloy tensile tests at elevated temperatures shows that the alloy exhibits HSRS. Deformation of more than 250% was obtained at temperatures above 650°C, at a strain rate of $10^{-2}\ s^{-1}$, which is two orders of magnitude higher than the strain rate for superplastic deformation of this alloy in the microcrystalline state.[16] Moreover, this alloy showed elongation of more than 200% at a strain rate of $10^{-1}\ s^{-1}$, and a temperature of 725°C. It is noteworthy that the maximum elongation (more than 500%) was obtained after HPT at a strain rate of $10^{-4}\ s^{-1}$ and a temperature of 650°C, which is $\sim 0{\cdot}4T_m$ where T_m is the melting temperature in degrees Kelvin. Stress–strain curves for the alloy after HPT show high strain hardening at strain rates above $10^{-4}\ s^{-1}$ (Fig. 4). A common explanation for strain hardening during superplasticity is concurrent grain growth because of the grain size dependence of superplastic flow. With this in mind, the grain growth related strain hardening is expected to be

Published by Maney Publishing (c) IOM Communications Ltd

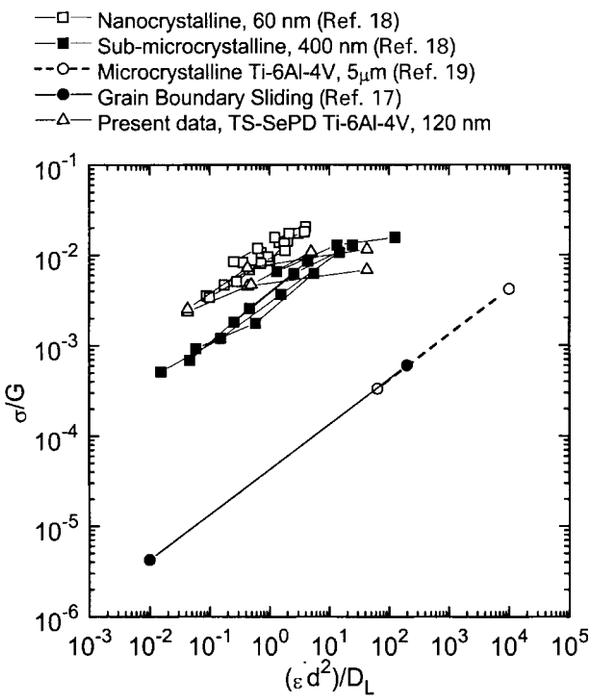

5 Flow stress normalised by modulus as function of strain rate normalised by grain size and diffusivity for Ti–6Al–4*X* alloys

greater at lower strain rates because more grain growth per unit strain would occur. Values for the strain rate sensitivity m were determined to be 0·38 to 0·42 in the strain rate range 10^{-4}–10^{-3} s^{-1} at 650°C for the alloy processed by both routes. The m values decrease down to 0·2 at higher strain rates. The activation energy determined from the slope of the log $\dot{\varepsilon}$ versus $1/T$ curves was 270 kJ mol^{-1}, which is much higher than that for grain boundary (97 kJ mol^{-1}) and lattice (153 kJ mol^{-1}) diffusion in Ti. This value is close to the activation energy of power law creep in Ti, which has been reported to be 242 kJ mol^{-1} (Ref. 17).

The development of ultrafine grain structures by HPT led to HSRS in a commercial Ti–6Al–4V alloy. But the deformation behaviour of such an alloy is quite different from the microcrystalline superplastic alloy. Sherby and Wadsworth[17] have proposed a phenomenological relationship that fits the experimental data for superplasticity in microcrystalline Ti–6Al–4V alloys quite well. The phenomenological relationship is given as[17]

$$\dot{\varepsilon} = 5 \times 10^9 \left(\frac{D_L}{d^2}\right)\left(\frac{\sigma}{E}\right)^2 \quad \ldots\ldots\ldots\ldots \quad (2)$$

where $\dot{\varepsilon}$ is the strain rate, D_L is the lattice diffusion coefficient, E is the Young's modulus, d is the grain size, and σ is the applied stress. Figure 5 shows a plot of ε versus $\dot{\varepsilon}d^2/D_L$ to compare the experimental kinetics of deformation in Ti–6Al–4V alloys with different grain sizes with the phenomenological relationship in equation (2). The data from Salishchev *et al.*[10,11] for nanocrystalline and sub-microcrystalline Ti–6Al–4Mo alloys and Meier *et al.*[20] for microcrystalline Ti–6Al–4V are also included in Fig. 5. The noteworthy aspect is that while the data for the microcrystalline state corresponds well with equation (2), the ultrafine grained materials show slower kinetics. This is interesting in view of the various discussions in the literature on the possibility of enhanced superplasticity in nanocrystalline alloys. While refinement in grain size does lead to lower superplastic temperatures at comparable strain rates, the kinetics is clearly slower on a normalised basis. The implication is that a simple extrapolation to the nanocrystalline range using the constitutive relationship for micrograin superplasticity is not going to work.

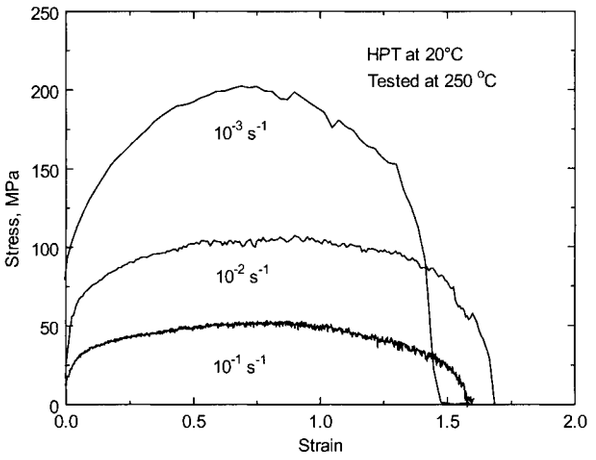

6 Stress–strain curves for nanocrystalline 1420 Al alloy processed by HPTS

NANOCRYSTALLINE SUPERPLASTICITY

A significant level of superplasticity has been observed in nanocrystalline Ni_3Al, and 1420 Al alloy (Al–Mg–Li) processed by HPT.[21] Experimental observations include both high strain rate and low temperature superplasticity. High strain rate superplasticity was observed in the 1420 Al alloy at temperatures as low as 250°C. These results

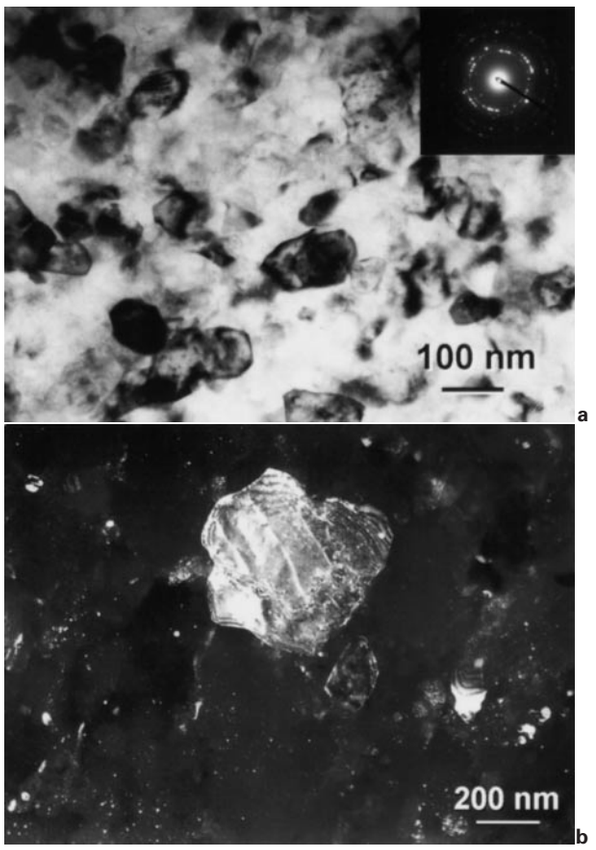

7 *a* bright field TEM of 1420 Al alloy as processed by severe plastic deformation and *b* dark field TEM of 1420 Al alloy after superplastic deformation to ~325% elongation at 250°C and strain rate of 1×10^{-1} s^{-1}

Published by Maney Publishing (c) IOM Communications Ltd

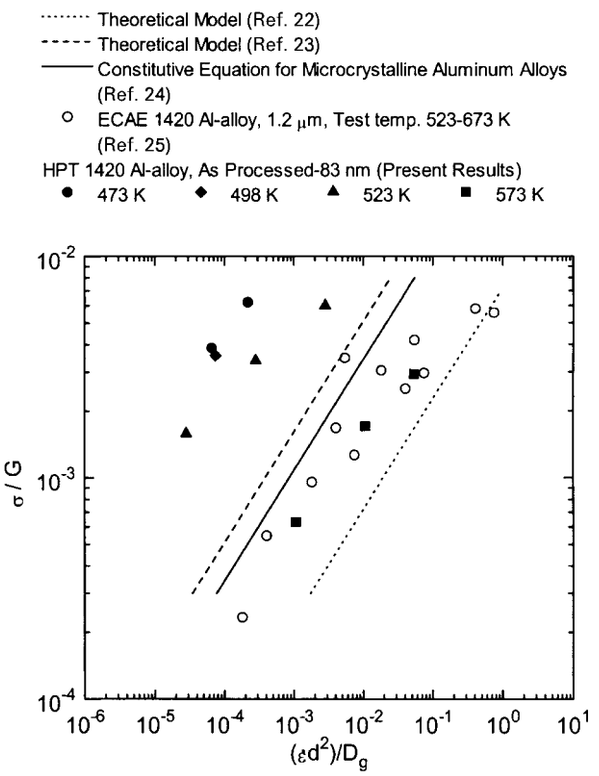

8 Flow stress normalised by modulus as function of strain rate normalised by grain size and diffusivity for 1420 Al alloy: three constitutive models are also plotted to demonstrate difference in flow stress between nanocrystalline and microcrystalline material

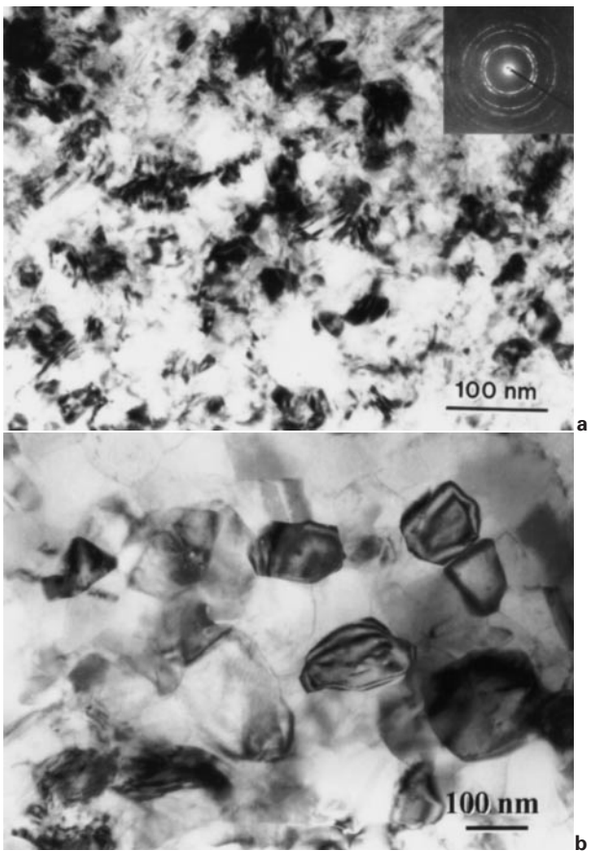

9 Bright field TEM images of Ni_3Al *a* as processed by severe plastic deformation and *b* after superplastic deformation at 650°C

are compared with those obtained from microcrystalline 1420 Al in Table 1. An elongation of ~390% was taken as a frame of reference. At 300°C, the strain rate was increased from 1×10^{-3} to 5×10^{-1} s^{-1} by grain size refinement from 6 μm to 100 nm. Stress–strain curves for nanocrystalline 1420 Al are shown in Fig. 6. Bright field TEM of the HPT as processed microstructure is shown in Fig. 7*a*, while Fig. 7*b* shows dark field TEM after superplastic deformation at 250°C and a strain rate of 10^{-1} s^{-1}. From Fig. 7*b* it is apparent that grain growth occurred in the 1420 Al alloy even at the lowest superplastic temperatures. After deformation at 250°C, the grain size was submicrocrystalline.

The effect of increasing temperature on the superplastic behaviour of nanocrystalline 1420 Al is shown in Fig. 8, which is a plot of modulus normalised stress as a function of strain rate normalised by grain size and diffusivity. Superimposed on this plot are lines corresponding to three constitutive models of superplasticity. From 200 to 250°C (473 to 523 K) the behaviour of nanocrystalline 1420 Al is clearly distinct from microcrystalline 1420 Al. At 300°C (573 K) the behaviour merges with that of microcrystalline material because of rapid grain growth.

Table 1 Comparison of superplastic results for 1420-Al

	100 nm grain size	1·2 μm grain size (data from Ref. 18)	6 μm grain size (data from Ref. 19)
Elongation, %	390	380	400
Temperature, °C	300	300	450
Strain rate (s^{-1})	5×10^{-1}	1×10^{-1}	1×10^{-3}
Flow stress at 50% strain, MPa	220	88	6

Nanocrystalline Ni_3Al, processed by HPT, demonstrated a significant lowering of the superplastic temperature compared with the microcrystalline material.[12] For an equivalent elongation of 460%, the superplastic temperature was reduced from 1050 to 725°C. This result introduced the possibility of forming structural intermetallics with conventional dies and tooling, such as those used to form Ti alloys. The HPT as processed microstructure is shown in Fig. 9*a*, while Fig. 9*b* shows the microstructure after deformation at 650°C. From Fig. 9*b*, it is apparent that the grain size after deformation was 100 nm or less. The

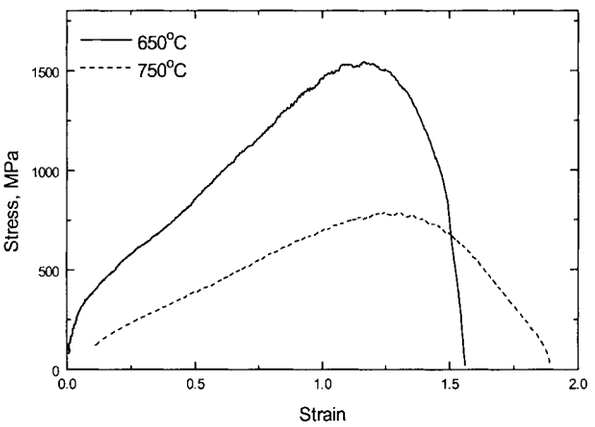

10 Stress–strain curves for nanocrystalline Ni_3Al deformed at constant strain rate of 10^{-3} s^{-1}: very high flow stresses are unusual for superplastic flow

Published by Maney Publishing (c) IOM Communications Ltd

comparatively greater stability of grain size is attributed to preferred atomic pairing in the ordered structure.

One of the general features of nanocrystalline superplasticity is high flow stress. The stress–strain curves in Fig. 10 demonstrate very high flow stresses in nanostructured Ni_3Al. Although the well-known temperature dependent strength anomaly and strong strain hardening in Ni_3Al occur near the test temperature of 725°C reported for the present work, a ductility minimum of the order of 20% elongation also occurs at this temperature for microcrystalline Ni_3Al.[26] Furthermore, fine grained specimens (2·9–9·5 μm) have not shown the strength anomaly.[27] Therefore, the stress anomaly alone is not sufficient to account for the observed behaviour, particularly in the light of the large elongation achieved. High flow stresses are apparent in nanocrystalline Ni_3Al even when normalised by grain size and diffusivity.[12] Higher normalised flow stresses are also apparent in nanocrystalline 1420 Al alloy as shown in Fig. 8. This leads to the conclusion that nanocrystalline superplasticity is not a simple extension of microcrystalline superplasticity scaled by grain size.

Conclusions

In microcrystalline materials where the grain size is stabilised by particles, the activation energy for high strain rate superplasticity changes with particle size. Diffusional relaxation models can be used to explain this change as well as predicting the temperature for the onset of high strain rate superplasticity in mechanically alloyed Ni or Al based alloys.

Nanostructured materials can offer enhancements of superplastic properties such as an increase in superplastic strain rate or a decrease in superplastic temperature. The large driving force for grain growth in these materials results in strain-enhanced grain enlargement during testing. The limited grain growth observed in nanocrystalline Ni_3Al has been attributed to the kinetic barrier of preferred atomic pairing in the ordered structure. Comparison of nanocrystalline and microcrystalline superplasticity indicates that nanocrystalline behaviour is not a simple extension of microcrystalline behaviour scaled by grain size.

Acknowledgements

This work was supported by a grant from the US National Science Foundation: grant no. NSF–DMR–9903321.

References

1. A. K. MUKHERJEE, R. S. MISHRA, and T. R. BIELER: *Mater. Sci. Forum*, 1997, **217**, 233.
2. T. MORI, M. OKABE, and T. MURA: *Acta Metall.*, 1980, **28**, 319.
3. A. K. MUKHERJEE, T. R. BIELER, and A. CHOKSHI: 'Materials architecture', (ed. J. B. Bilde-Sorensen *et al.*), 207; 1989, Roskilde, Riso National Laboratory.
4. R. C. KOLLER and R. RAJ: *Acta. Metall.*, 1978, **26**, 1551.
5. H. J. FROST and M. F. ASHBY: 'Deformation mechanism maps', 164; 1982, London, Permagon.
6. R. F. SINGER and G. H. GESSINGER: in 'Deformation of polycrystals: mechanism and microstructures', (ed. N. Hansen *et al.*), 385; 1995, Roskilde, Riso National Laboratory.
7. R. F. SINGER and G. H. GESSINGER: 'Deformation of polycrystals', (ed. N. Hansen *et al.*), 365; 1981, Roskilde, Riso National Laboratory.
8. J. K. GREGORY, J. C. GIBELING, and W. D. NIX: *Metall. Trans. A*, 1985, **16A**, 777.
9. R. S. MISHRA, T. R. BIELER, and A. K. MUKHERJEE: *Acta. Mater.*, 1997, **45**, 561.
10. G. A. SALISHCHEV, O. R. VALIAKHMETOV, V. A. VALITOV, and S. K. MUKHTAROV: *Mater. Sci. Forum*, 1994, **170–172**, 121.
11. G. A. SALISHCHEV, R. M. GALEYEV, S. P. MALYSHEVA, and O. R. VALIAKHMETOV: *Mater. Sci. Forum*, 1997, **243–245**, 585.
12. R. S. MISHRA, R. Z. VALIEV, S. X. MCFADDEN, R. K. ISLAMGALIEV, and A. K. MUKHERJEE: *Mater. Sci. Eng. A*, 1998, **252**, 174.
13. D. W. KUM, W. J. KIM, and G. FROMMEYER: *Scr. Mater.*, 1999, **40**, 223.
14. R. Z. VALIEV, D. A. SALIMONENKO, N. K. TSENEV, P. B. BERBON, and T. G. LANGDON: *Scr. Mater.*, 1997, **37**, 1945.
15. R. Z. VALIEV, E. V. KOZLOV, YU. F. IVANOV, J. LIAN, A. A. NAZAROV, and B. BAUDELET: *Acta Metall. Mater.*, 1994, **42**, 2467.
16. O. A. KAIBYSHEV: 'Superplasticity of alloys, intermetallics, and ceramics', 317; 1992, Berlin, Heidelberg, Springer-Verlag.
17. O. D. SHERBY and J. WADSWORTH: *Prog. Mater. Sci.*, 1989, **33**, 169.
18. G. A. SALISCHEV, R. M. GALEYEV, S. P. MALISHEVA, and O. R. VALIAKHMETOU: *Mater. Sci. Forum*, 1996, **243–245**, 585.
19. M. L. MEIER and A. K. MUKHERJEE: *Scr. Metall. Mater.*, 1991, **25**, 1471.
20. M. L. MEIER, D. R. LEUSER, and A. K. MUKHERJEE: *Mater. Sci. Eng. A*, 1992, **154**, 165.
21. S. X. MCFADDEN, R. S. MISHRA, R. Z. VALIEV, A. P. ZHILYAEV, and A. K. MUKHERJEE: *Nature*, 1999, **398**, 684.
22. A. BALL and M. M. HUTCHISON: *Met. Sci. J.*, 1969, **3**, 1.
23. A. K. MUKHERJEE: *Mater. Sci. Eng.*, 1971, **8**, 83.
24. R. S. MISHRA, T. R. BIELER, and A. K. MUKHERJEE: *Acta Metall. Mater.*, 1995, **43**, 877.
25. P. B. BERBON, N. K. TSENEV, R. Z. VALIEV, M. FURUKAWA, Z. HORITA, M. NEMOTO, and T. G. LANGDON: *Metall. Mater. Trans.*, 1998, **29A**, 2237.
26. C. T. LIU and V. SIKKA: *J. Met.*, 1996, **38**, 19.
27. E. M. SCHULSON, I. BAKER, and H. J. FROST: in 'High temperature ordered intermetallic alloys II', (ed. N. S. Stoloff), MRS Symp. Proc., Vol. 81, 195; 1987, Warrendale, PA, Materials Research Society.

Published by Maney Publishing (c) IOM Communications Ltd